Transcriptional profiling of the terpenoid biosynthesis pathway and *in vitro* tests reveal putative roles of linalool and farnesal in nectarine resistance against brown rot

Authors: Marta Balsells-Llauradó[1], Núria Vall-llaura[1], Josep Usall[1], Christian J. Silva[2], Barbara Blanco-Ulate[2], Neus Teixidó[1], Maria Caballol[1], Rosario Torres[1]*

(1) IRTA, Postharvest Programme, Edifici Fruitcentre, Parc Científic i Tecnològic Agroalimentari de Lleida, Parc de Gardeny, 25003 Lleida, Catalonia, Spain

(2) Department of Plant Sciences, University of California, Davis, Davis, CA 95616, United States

*Corresponding author: Rosario Torres (rosario.torres@irta.cat)

Official email addresses of all authors: Marta Balsells-Llauradó (marta.balsells@irta.cat), Núria Vall-llaura (nuria.vall-llaura@irta.cat), Josep Usall (josep.usall@irta.cat), Christian J. Silva (cjsilva@ucdavis.edu), Barbara Blanco-Ulate (bblanco@ucdavis.edu), Maria Caballol (maria.caballol@udl.cat), Neus Teixidó (neus.teixido@irta.es).

Keywords: *Monilinia*, stone fruit disease, fruit developmental stage, secondary metabolism, terpenoids, postharvest

Abstract

The most devastating fungal disease of peaches and nectarines is brown rot, caused by *Monilinia* spp. Among the many plant responses against biotic stress, plant terpenoids play essential protective functions, including antioxidant activities and inhibition of pathogen growth. Herein, we aimed to characterize the expression of terpenoid biosynthetic genes in fruit tissues that presented different susceptibility to brown rot. For that, we performed artificial inoculations with *Monilinia laxa* at two developmental stages (immature and mature fruit) of two nectarine cultivars ('Venus' –mid-early season cultivar - and 'Albared' –late season cultivar-) and *in vitro* tests of the key compounds observed in the transcriptional results. All fruit were susceptible to *M. laxa* except for immature 'Venus' nectarines. In response to the pathogen, the mevalonic acid (MVA) pathway of the 'Venus' cultivar was highly induced in both stages rather than the methylerythritol phosphate (MEP) pathway, being the expression of some MEP-related biosynthetic genes [e.g., *PROTEIN FARNESYLTRANSFERASE (PpPFT),* and *3S-LINALOOL SYNTHASE (PpLIS*)] different between stages. In 'Albared', both stages presented similar responses to *M. laxa* for both pathways. Comparisons between cultivars showed that *HYDROXYMETHYLGLUTARYL-CoA REDUCTASE (PpHMGR1)* expression levels were common in susceptible tissues. Within all the terpenoid biosynthetic pathway, linalool- and farnesal-related pathways stood out for being upregulated only in resistant tissues, which suggest their role in mediating the resistance to *M. laxa.* The *in vitro* antifungal activity of linalool and farnesol (precursor of farnesal) revealed fungicidal and fungistatic activities against *M. laxa*, respectively, depending on the concentration tested. Understanding the different responses between resistant and susceptible tissues could be further considered for breeding or developing new strategies to control brown rot in stone fruit.

1. Introduction

Stone fruit comprise species of the *Prunus* genus, which includes over 400 to 430 species [1], such as apricots, cherries, peaches, nectarines, and plums. Peaches and nectarines are the fifth most important fruit crop within the Rosaceae family [2], with a global production of 25.7 million tons in 2019 [3]. During harvest and postharvest, stone fruit are generally susceptible to fungal diseases, particularly to infections caused by *Monilinia* spp., the etiological agent of brown rot [4]. The main pathogenic *Monilinia* species in stone fruit are *M. laxa*, found worldwide [5], and *M. fructicola,* which is more virulent [6] but only restricted to Australasia, North and South America [7], and Europe since 2001 [8]. *Monilinia* spp. can infect fruit without naturally occurring entry points [9] at any developmental stage, although brown rot susceptibility increases dramatically during maturation [10]. Meanwhile, the fungus can establish latent or quiescent infections until optimal conditions trigger the disease cycle [11].

In response to fungal attack, nectarine fruit activates different signaling pathways (e.g., oxidative burst and hormone signaling), leading to the expression of pathogenesis-related proteins and accumulation of secondary metabolites, among others [12]. Secondary metabolites are involved in fruit defenses as constitutive or inducible responses [13]. Among them, terpenoids represent the largest and most diverse class of secondary metabolites, known to play defense roles against abiotic stress (e.g., UV-B light) [14] and various biotic interactions [15]. For instance, monoterpenes, triterpenes, sesquiterpenes, and terpene glycosides are accumulated at all stages of noble rot caused by *Botrytis cinerea* in ripe grape berries [16]. Quilot-Turion et al. [17] found that up to 30 phenolic and terpenoid compounds of peach were released in response to wounding and inoculation with *M. laxa.* Nevertheless, there are no studies aiming to decipher the regulation of the terpenoid biosynthetic pathway during the interaction between *Monilinia* spp. and unwounded nectarines.

All terpenoids are derived from the five-carbon (C5) precursor isopentenyl diphosphate (IPP) and its double-bond isomer dimethylallyl diphosphate (DMAPP) [18]. Their biosynthesis mainly comes from two pathways; the cytosolic mevalonic acid (MVA) pathway, which predominantly provides the precursors for sesquiterpenoids, steroids, and triterpenoids, and

the plastidial methylerythritol phosphate (MEP) pathway, which supplies precursors for hemiterpenoids, monoterpenoids, diterpenoids and carotenoids [18]. The 3-hydroxy-3-methylglutaryl-CoA (HMG) synthase (HMGS) and HMG reductase (HMGR) are the rate-limiting steps of the MVA pathway [19,20], whereas the 1-deoxy-D-xylulose 5-phosphate synthase (DXS) is considered the regulator of the MEP pathway [21]. Knowledge about the regulation and dynamics of the MVA and MEP pathways during fruit-pathogen interactions will help resolve the relevance of particular terpenoids in fruit resistance or susceptibility to fungal disease.

In a recent publication, we observed that several genes involved in terpenoid metabolism were significantly induced after *M. laxa* inoculation of resistant immature nectarines (cv. 'Venus') when compared to susceptible mature fruit (cv. 'Venus') [12]. Here, we assessed the disease development followed by a detailed transcriptional analysis of the terpenoid biosynthetic pathway in healthy and *M. laxa*-inoculated tissues of two nectarine cultivars, 'Venus' and 'Albared', which present differences in susceptibility to brown rot according to their developmental stage [22]. We then focused on specific terpenoid biosynthetic genes that displayed differential expression between cultivars and developmental stages, and that could explain the resistance or susceptibility outcomes observed. Finally, and to validate the gene expression results, we also tested the *in vitro* antifungal activity of two specific nectarine terpenoid compounds (linalool and farnesol) on *M. laxa* growth. These genes and compounds should be further considered for functional analyses and targets for future breeding or management strategies against brown rot.

2. Materials and methods

2.1. Plant material and fungal culture

Two cultivars of nectarine (*P. persica* var. *nucipersica* (Borkh.) Schneider) were used for the experiments. 'Venus' and 'Albared' nectarines were obtained from organic orchards located in Lleida (Catalonia, Spain). To avoid the naturally occurring inoculum, fruit were bagged at least 6 weeks before the commercial harvest. Fruit was harvested at two different

101 developmental stages, based on grower's recommendations: "immature" (184 and 219 Julian
102 days for 'Venus' and 'Albared' cultivars, respectively) and "mature" (211 and 246 Julian days
103 for 'Venus' and 'Albared' cultivars, respectively). For each sampling, fruit was homogenized
104 using a DA-Meter (TR-Turoni, Forli, Italy), based on the single index of absorbance difference
105 (I_{AD} = 1.99–2.26 and 1.00–2.06 for immature fruit and I_{AD} = 0.25–1.60 and 0.16–1.32 for
106 mature fruit, for 'Venus' and 'Albared' cultivars, respectively). Flesh firmness was measured
107 on 20 randomly fruit at harvest day, following the previously described protocol [23]. The
108 fungal strain used for all experiments was the *M. laxa* single-spore strain 8L (ML8L, Spanish
109 Culture Type Collection number CECT 21100).
110
111 2.2. Fruit inoculations
112 Conidial suspensions were prepared as described previously by Baró-Montel et al. [24]. For
113 gene expression analyses of 'Albared' nectarines, six drops of 30 µL of conidial suspension
114 (10^6 conidia mL^{-1}) were applied on each fruit. Sterile water containing 0.01% (w/v) Tween-80
115 was used for mock-inoculated fruit (control). Fruit was incubated in containers in darkness
116 and with high relative humidity (97 ± 3% and 20 ± 1 °C). Three replicates consisting of five
117 fruit per treatment were obtained at each sampling point (6, 14, 24, 48, and 72 hpi).
118
119 2.3. RNA extraction and gene expression analysis
120 Gene expression analysis for terpenoid biosynthetic genes of 'Venus' cultivar was conducted
121 using the data of normalized read counts from a previous study conducted by our group [12].
122 Tissue sampling, extraction of total RNA, elimination of contaminant DNA, RNA concentration
123 and quality assessment, synthesis of first-strand cDNA, primer efficiency, and quantification
124 of gene expression through Real-Time Quantitative PCR (RT-qPCR) of cv. 'Albared' samples
125 were conducted following the same methodology described for cv. 'Venus' [12]. Fungal
126 biomass on cv. 'Albared' fruit determination was calculated based on the relative gene
127 expression of the *M. laxa ACTIN* (*MlACT*) reference gene normalized to the nectarine
128 *ELONGATION FACTOR 2* (*PpTEF2*) reference gene expression. Gene expression levels of

each gene of interest were normalized to *PpTEF2* [25], using the formula $2^{(\text{reference gene Ct} - \text{gene of interest Ct})}$ [26]. Primers (**Supplementary Table S1**) were retrieved from the literature [14,25,27] or designed *de novo.* The RNA-Seq expression profiles of nine terpenoid genes previously reported in the 'Venus' cultivar [12] were validated by RT-qPCR using the same tissues. The Person correlation values between RNA-Seq and RT-qPCR data was *R*: 0.75, *P* value = 2.58×10^{-20} (**Suppl. Table S2**).

2.4. Evaluation of the antifungal activity of terpenoid compounds on *in vitro M. laxa* growth

To test the antifungal activity on *M. laxa* growth of linalool and farnesol (precursor of farnesal), the pure compounds were purchased from Sigma-Aldrich (Madrid, Spain) and applied at several concentrations based on previous studies of our group (ranges from 1.00 to 0.01 mg mL^{-1} for a headspace or media). For linalool, 10 µL of conidial suspension of *M. laxa* (10^6 conidia mL^{-1}) were applied to the center of semi-synthetic peach juice based-medium plates (100 % of organic peach juice, 15 g L^{-1} of agar, pH = 4.0). A paper filter (75 mm diameter) with different aliquots of the compound (corresponding to 0.11, 0.05, 0.03, and 0.01 mg mL^{-1} for a headspace), were positioned inside the cover of the Petri dishes (85 x 85 mm), and immediately sealed with parafilm. Plates were incubated at 20 ± 1 ºC under complete darkness. To assess either the fungistatic or fungicide effect of the compound, colony diameter was measured after 3 days. Then, petri covers were replaced by new ones to cease the effect of the compound, and after 4 days, colony diameter measurements were conducted again. Dishes with a paper filter with sterile water at the maximum volume were used as control. The same methodology described for linalool was conducted for the farnesol assessment with some modifications. Conidial suspensions were applied on cellophane disks (85 mm) overlaid on peach juice based-medium plates containing different concentrations of pure farnesol (0.89, 0.44, 0.22, 0.11, and 0.06 mg mL^{-1} in the media). After 3 days, the cellophane containing *M. laxa* was transferred to new peach juice based-medium plates to stop the effect of the compound. Plates were then incubated for 4 additional days. Colony area was measured at 3 and 7 days using Inkscape™ software version 1.1

157 (https://inkscape.org). Plates without farnesol were used as controls. The percentage of
158 fungal growth inhibition was calculated after 3- and 7-days post-inoculation, following the
159 formula (%)=[(aC-aT)/aC)]·100, where aC is the diameter or area average of control and aT
160 is the diameter or area average of the plate containing farnesol or linalool. Both assays
161 consisted of three biological replicates for each compound. The experiments were conducted
162 twice.
163
164 2.5. Statistical analysis
165 Data were statistically analyzed with JMP® software version 16.0.0 (SAS Institute Inc., Cary,
166 NC, USA). Relative gene expression was subjected to analysis of variance (ANOVA). When
167 comparisons were conducted between two means (control *vs* inoculated), Student's *T*-test (*P*
168 ≤ 0.05) was used. For means comparison across time for each control and inoculated fruit
169 (normalized read counts or relative gene expression), or for *M. laxa* growth inhibition for each
170 concentration, Tukey's HSD test (*P* ≤ 0.05) was conducted.
171
172 **3. Results**
173 3.1. Fruit developmental stage and cultivar determine susceptibility to brown rot
174 Evaluation of the fungal disease in two nectarine cultivars at two different developmental
175 stages revealed that cv. 'Albared' was susceptible to *M. laxa* in both stages after 72 hpi
176 (**Figure 1**). In 'Venus' nectarines, *M. laxa* was only able to cause disease in mature fruit,
177 whereas no disease symptoms were observed in immature fruit (**Suppl. Figure S1**). Such
178 differences between immature stages could not rely on fruit quality attributes since both
179 stages were comparable between cultivars in terms of flesh firmness (N), in which values
180 were 108.8 ± 1.9 ('Venus') and 105.6 ± 1.7 ('Albared') for immature and 74.4 ± 2.7 ('Venus')
181 and 73.5 ± 2.3 ('Albared') for mature fruit.
182 The analysis of the fungal biomass (**Figure 1**) revealed that in immature 'Albared' nectarines,
183 fungal biomass of the inoculated tissues significantly peaked at 72 hpi, corresponding with
184 the visual symptoms of the disease. In inoculated mature fruit, the fungal biomass significantly

185 increased exponentially ($y = 0.6947e^{0.0636t}$, $R^2 = 0.8719$), paralleling the rotting of the pulp.
186 Remarkably, the fungal biomass in mature tissue was significantly higher than in the immature
187 fruit at all time points (**Figure 1**).
188
189 3.2. Terpenoid biosynthetic genes were differentially expressed in the 'Venus' cultivar in
190 response to *M. laxa*
191 An analysis of differentially expressed genes (DEGs) of our previous RNA-seq study,
192 conducted in 'Venus' cultivar [12], pointed out that among the total terpenoid-related DEGs,
193 up to 35% of the genes were related to terpenoid backbone, while steroid-related genes where
194 those less differentially expressed (**Figure 2a**). Venn's diagram showed the big divergence
195 between immature and mature tissues, for either up and down-regulated DEGs (**Figure 2b**).
196 Remarkably, the majority of up-regulated DEGs were common between tissues, whereas
197 those down-regulated DEGs were more abundant in mature nectarines. The (*3S)-LINALOOL*
198 *SYNTHASE* (*PpLIS2*) highlighted for being up-regulated only in immature tissue, while the
199 *HYDROXYMETHYLGLUTARYL-CoA REDUCTASE* (*HMGR*) and *the QUINONE*
200 *REDUCTASE* genes were the unique down-regulated genes in the immature tissue.
201 Normalized read counts from our previous RNA-Seq study [12] were used to depict the
202 expression patterns of the terpenoid biosynthetic genes in both control- and *M. laxa*-
203 inoculated 'Venus' fruit at two developmental stages (**Figure 3**). In control tissues, both
204 immature and mature fruit presented a similar gene expression pattern, with no significant
205 differences among developmental stages. Most of the genes significantly changed (i.e.,
206 increase, decrease, or only fluctuate) their expression along the incubation time course. The
207 RNA-Seq data revealed an evident response to *M. laxa* inoculation at both fruit developmental
208 stages.
209 Specifically, in the first steps of the terpenoid backbone biosynthesis (from *PpAACT* to
210 *PpMDS*) (the reader is referred to **Suppl. Table S1** for the full gene names), the presence of
211 the pathogen significantly upregulated the expression of the MVA pathway compared to
212 control tissues in both stages (**Figure 3**). In contrast, the MEP pathway was largely

downregulated. The average expression across time of *PpHMGS* and *PpHMGR1* in *M. laxa*-inoculated fruit compared to control was 2.22- and 1.44-fold higher, respectively, in immature tissues at 48 hpi, whereas both genes were up to 19.23 and 24.87-fold higher, respectively, in mature tissues at the same time point. In contrast, *PpDXS1* was 1.27-fold less expressed (average of 14 and 48 hpi) in immature fruit, 1.38-fold less expressed (average of 14 and 24 hpi) in mature tissues, compared to control.

The activation of the MVA pathway occurred faster in mature than immature fruit, as observed by the earlier induction of genes involved in MVA terpenoid backbone biosynthesis (e.g., *PpIDI, PpFPS, PpSQS*). Most of the biosynthetic genes that are downstream to farnesyl-PP and geranyl-PP were predominantly upregulated in *M. laxa*-inoculated fruit compared to control at both stages. Hence, results seemed to point out that the final targets of 'Venus' nectarines in response to *M. laxa* were steroids (e.g., *PpSQS* and *PpSM*), monoterpenoids (*PpLIS* and *PpND*), and triterpenoids *(PpAS*). Overall, paralogs within each gene family behaved similarly, except for *LIS*, in which *PpLIS1* and *PpLIS2* paralogs remained downregulated to increase thereafter in immature fruit. On the contrary, in mature fruit, *PpLIS1* expression was, in average, 1.39-fold higher, whereas *PpLIS2* was 1.85-fold less expressed (average of 24 and 48 hpi) in response to *M. laxa* compared to control. On the other side, sesquiterpenoid biosynthetic genes (*PpPFT* and *PpFOLK*) in inoculated tissues were significantly downregulated compared to controls in mature fruit and only upregulated at early time points (6 or 14 hpi) in immature fruit.

3.3. *Monilinia laxa* induces the expression of the terpenoid backbone and steroid biosynthetic genes in the 'Albared' cultivar

Potential candidate genes of terpenoid biosynthesis (MVA pathway and downstream genes) in 'Venus' cultivar, which were largely induced in response to *M. laxa* in both developmental stages, were selected for expression analysis in the 'Albared' cultivar. The expression levels of two genes of the MVA pathway (*PpHMGS* and *PpHMGR1*) and two other backbone terpenoid biosynthetic genes (*PpIDI* and *PpFPS2*) were lower (< 0.3 relative expression) in

controls compared to *M. laxa*-inoculated fruit, and overall similar between immature and mature tissues (**Figure 4**). Although the expression of *PpHMGR1* did not show a clear pattern in both stages across time, and the expression of *PpFPS2* in immature fruit tended to decrease through time, other genes (*PpHMGS* and *PpIDI* in both stages and *PpFPS2* in mature fruit) showed a steadily expression across the time points.

In *M. laxa*-inoculated immature fruit, *PpHMGS* expression remained steadily across most time points and was later significantly downregulated (3.7-fold less) at 72 hpi compared to control. *PpHMGR1* was significantly activated by the pathogen from 14 hpi onwards, displaying an upregulation of 11.9-fold at 72 hpi (**Figure 4a, b**). *PpIDI* was significantly upregulated later in time in immature tissues (1.6 and 2.1-fold higher at 48 and 72 hpi, respectively, compared to the control), whereas *PpFPS2* was significantly induced by the pathogen at some time points (2.6 and 2.3-fold higher at 14 and 48 hpi, respectively, compared to control) (**Figure 4c, d**). The relative gene expression in *M. laxa*-inoculated mature fruit revealed a similar pattern to that in immature fruit. The unique significant downregulation of *PpHMGS* in inoculated tissues compared to control (3-fold less) occurred earlier (at 24 hpi) than that in immature, whereas *M. laxa* inoculation significantly increased the *PpHMGR1* expression (up to 14.8 and 11.1-fold higher at 48 and 72 hpi, respectively) compared to control since 14 hpi onwards (**Figure 4a, b**). The relative expression of *PpIDI* and *PpFPS2* in mature inoculated fruit was significantly higher than control fruit through time (from 14 to 48 hpi), being, on average, 2.9 and 8.9-fold more expressed, respectively (**Figure 4c, d**).

Several groups of compounds can be derived from the terpenoid backbone. Relative expression levels of steroid biosynthetic genes (*PpSQS* and *PpSM2*) in control 'Albared' fruit were scarce (< 0.17 relative expression) compared to *M. laxa*-inoculated tissues and non-statistically significant between developmental stages (**Figure 5**). Besides, the relative expression fluctuated across time in both tissues. In contrast, in *M. laxa*-inoculated immature fruit, the presence of the pathogen significantly induced the expression of *PpSQS* later in time (1.9 and 2.7-fold change at 48 and 72 hpi, respectively, compared to controls), paralleling the spread of the disease (**Figure 5a**). *Monilinia laxa* inoculation also induced the expression of

PpSM2 since 24 hpi onwards (an average of 4.9-fold change until 72 hpi) (**Figure 5b**). In mature tissues, the induction of the expression of *PpSQS* and *PpSM2* triggered by *M. laxa* inoculation occurred earlier (since 14 hpi), similarly to *PpIDI* and *PpFPS2*, both displaying a significant higher expression in inoculated tissues compared to control, being 12 and 44.7-fold higher for *PpSQS* and *PpSM2*, respectively, at 48 hpi.

3.4. Expression of genes in the sesquiterpenoid and monoterpenoid pathways is differentially induced by *M. laxa* in the 'Albared' cultivar

Within the sesquiterpenoid family, gene expression of farnesal biosynthetic genes were downregulated across time and due to *M. laxa* inoculation (**Figure 6**). Relative expression of *PpPFT1*, *PpSIMT,* and *PpFOLK* genes in control 'Albared' nectarines were low (< 0.16 relative expression) compared to the other genes analyzed, and their expression patterns differed across time. In detail, *PpPFT1* and *PpFOLK* expression in immature control fruit significantly increased from 14 to 72 hpi (4.7 and 3.3-fold, respectively) (**Figure 6a, c**). In contrast, levels of *PpSIMT* in control fruit remained steady across time in both stages (**Figure 6b**).

In *M. laxa*-inoculated immature fruit, the relative expression of *PpPFT1* at the beginning (6 hpi) and at the end (72 hpi) of the infection course was significantly reduced (up to 3.1-fold less) compared to control fruit (**Figure 6a**). The expression of *PpFOLK* was downregulated (up to 6.9-fold) at 72 hpi compared to controls, coinciding with the spread of the tissue maceration (**Figure 6c**). In *M. laxa*-inoculated mature fruit, both *PpPFT1* and *PpFOLK* expressions were also predominantly downregulated compared to controls. However, such reduction occurred from 24 to 48 hpi (in average, 2.6 and 2.4-fold less for each gene, respectively). Remarkably, *M. laxa*-inoculation caused no significant effect in the expression levels of *PpSIMT* compared to controls across time (**Figure 6b**).

Regarding monoterpenoid biosynthesis, the expression pattern of genes codifying for 3S-linalool synthase (*PpLIS1* and *PpLIS2*) depended on the developmental stage analyzed (**Figure 7**). Overall, in the control fruit, expression levels of the paralog *PpLIS1* were higher (up to 1.2-fold) than *PpLIS2* (up to 0.05-fold). The relative expression of *PpLIS1* was

297 significantly higher in mature fruit (average of 0.75-fold) than immature fruit (average of 0.1-
298 fold) (**Figure 7a**). Remarkably, whereas the expression of *PpLIS1* in control immature fruit
299 significantly peaked at 72 hpi, *PpLIS2* expression significantly changed throughout time,
300 although with no clear pattern. Regarding fruit inoculated with *M. laxa, PpLIS1* also displayed
301 a higher gene expression level in both stages than *PpLIS2*; however, *PpLIS2* expression was
302 more impacted by *M. laxa* inoculation across time (**Figure 7b**). The presence of the pathogen
303 in the immature fruit significantly reduced by 1.8-fold *PpLIS1* expression compared to control
304 fruit only at 72 hpi, while significantly increased by 2.7-fold the expression in mature fruit at 6
305 hpi, when compared to the control (**Figure 7a**). *Monilinia laxa* inoculation significantly induced
306 the expression of *PpLIS2* in the immature tissues at 14 hpi and then caused a significant
307 reduction in expression levels up to 6.4-fold at 72 hpi compared to controls (**Figure 7b**). In
308 contrast, in *M. laxa*-inoculated mature fruit, *PpLIS2* was already significantly reduced by 3.3-
309 fold at 24 hpi compared to control.
310
311 3.5. Linalool and farnesol have antifungal and fungistatic properties
312 Based on the transcriptomics results, the biosynthesis of linalool and farnesol appear to be
313 associated with resistance against *M. laxa* in nectarine. To determine if these compounds are
314 antifungal or fungistatic, we evaluated the growth of *M. laxa in vitro* culture when exposed to
315 various concentrations of linalool and farnesol. Results showed that linalool had a fungicide
316 effect at the highest concentration tested (0.11 mg mL^{-1} headspace) (**Table 1**). At
317 concentrations below 0.05 mg mL^{-1} of linalool, *M. laxa* growth was inhibited between 65.5 –
318 89.3 % at 3 days. However, the fungal growth was recovered after removing the compound,
319 thus revealing that it possesses a fungistatic effect (**Table 1**). Farnesol also inhibited *M. laxa*
320 growth, but after removing the compound, the fungal growth was completely recovered,
321 irrespective of the concentration. Thus, farnesol only presented a fungistatic effect at all
322 concentrations tested (**Table 1**).
323

4. Discussion

The fruit host defense responses and the virulence strategies displayed by the pathogen during the nectarine-*M. laxa* interaction are starting to be unveiled. Our previous RNA-Seq study [12] pointed out the possible involvement of nectarine terpenoids metabolism in response to *M. laxa*. However, to the best of our knowledge, there are no studies reporting the role of nectarine terpenoids in resistance or susceptibility to brown rot. Here, we deepen into this metabolism by analyzing its expression on different nectarine tissues displaying different brown rot susceptibility, as well as determining the effect of different terpenoid products on the development of *M. laxa*. Recently, Muto et al. [28] reported the terpenoid profiles of eight nectarine and peach cultivars (without fungal infection), at both gene expression (e.g., *PpLIS2* and *PpAFS*) and metabolite levels. In our work, the expression levels of the terpenoid biosynthetic genes in healthy tissues (controls) of both nectarine cultivars were like those reported by Muto et al. [28].

Based on our results, *M. laxa* infections behaved differently between cultivars at the immature stage. Although it is generally accepted that the pathogen can infect fruit at any growth stage [10], the disease did not progress in 'Venus' immature fruit. *Monilinia laxa* was still active in the immature 'Venus' fruit since a peak on the fungal biomass occurred at 14 hpi, deaccelerating afterward, probably due to a shift to a quiescent or autolytic state [12]. In this work and contrary to that observed in the 'Venus' cultivar, *M. laxa* managed to infect immature 'Albared' nectarines. Such disease progression was also evident when analyzing the fungal biomass since it progressively increased across time and significantly peaked at 72 hpi, when the disease symptoms were most visible.

Many factors, including those climatological or intrinsic to the host itself, can influence brown rot progression. In fact, conidia of *Monilinia* spp. can remain quiescent until favorable factors trigger the disease [29]. Although fruit physical attributes could influence fruit susceptibility to pathogens and hence they should not be obviated, the results from our study demonstrated that there were no significant differences among cultivars within each developmental stage

for flesh firmness (e.g., an important parameter associated with fungal susceptibility). Thus, differences in brown rot susceptibility among ‘Venus’ and ‘Albared’ should be derived from additional fruit genetic and compositional characteristics. Hence, identifying molecular pathways and genes that differ between resistant tissues (i.e., immature 'Venus') and susceptible ones (both tissues of ‘Albared’ and mature ‘Venus’ nectarines) can provide clues about the main host factors driving resistance and susceptibility to brown rot.

‘Venus’ nectarines, irrespective of the fruit developmental stage, mainly activated the MVA and not the MEP pathway to respond against *M. laxa*. In fact, the plastidial pathway was downregulated in response to the pathogen. Which pathway is activated depends on the stimuli to which the plants are submitted, and consequently, the need for specific end-compounds to properly face the stress. Under pathogen attack, plant cells can induce the MVA pathway to direct the flux toward the production of sesquiterpenes, known to exhibit antifungal activities [18]. For instance, some sesquiterpenes (β-elemene from rice) exhibit antifungal activity against *Magnaporthe oryzae* [30]. Both *HMGS* and *HMGR* are considered key regulatory genes of the MVA pathway [19,20]. The expression of HMGR family members depends on several factors, including the fruit developmental stage, plant tissue, and external stimuli (e.g., pest and pathogen attack) [20,31]. Many studies have reported the overall control of *HMGR* genes to the steroid pathway, which often depends on individual genes of *HMGR* families (i.e., *HMGR1* and *HMGR2* differentially regulate the phytosterols and sesquiterpenoids production, respectively [20]). However, under biotic stresses, individual *HMGR* genes direct the flux towards the production of stress-induced compounds. For instance, the fungal elicitor arachidonic acid induces the *SlHMGR2* expression and carotenoid production (lycopene) in young and mature tomatoes [32]. In our work, the upregulation of *PpHMGR1* in susceptible tissues (both stages of ‘Albared’ and mature ‘Venus’ fruit) could act by directing the flux towards steroid synthesis. In addition to the primary function of steroids as membrane structure compounds and regulators of growth and development [18], steroids such as phytosterol stigmasterol (the end-product of the

steroid pathway) are involved in plant-pathogen interactions, as reported for *Arabidopsis thaliana–Pseudomonas syringae* [33]. Besides, its precursor (β-sitosterol) is accumulated in infected berries with *B. cinerea* [34]. In our work, the expression of steroid biosynthetic genes was induced by the pathogen in all inoculated tissues (both stages of both cultivars) along with the infection progression.

Overall, terpenoid metabolism was induced in susceptible and resistant nectarine tissues; however, some specific pathways (i.e., farnesal-related genes) were almost not activated in susceptible fruit. The overall downregulation of farnesal-related pathway (e.g., *PpPFT* and *PpFOLK*) in susceptible tissues (i.e., mature 'Venus' and both tissues of 'Albared' nectarines) (**Figure 3 and 6, Table 2**) suggest that these genes may be repressed by the pathogen in the susceptible tissues. In this line, the upregulation at the beginning of the infection in resistant immature 'Venus', coinciding with the highest fungal biomass on the fruit surface [12], pointed out a putative role towards plant protection, since, in these tissues, *M. laxa* failed in causing disease. Although farnesal has only shown antimicrobial activity against human pathogens [35,36], the application of farnesol to pepper leaf discs has been shown to reduce the aphid populations [37]. Here, we tested for the first time the *in vitro* antifungal activity of farnesol against *M. laxa* and found that this compound has a fungistatic activity. Hence, both gene expression and antifungal activity results lead us to hypothesize that farnesal contributed to resistance in immature 'Venus' tissues, while the reduced expression of this biosynthetic pathway in the susceptible tissues led to an enhanced susceptibility.

The upregulation of *PpLIS* paralogs in resistant tissues after 14 hpi and downregulation in susceptible tissues at some time points (**Figure 3 and 7, Table 2**) suggested that linalool synthase expression could be implicated in protective functions, either through signaling or direct implication of the linalool product. Under various conditions, the cytosolic MVA and plastidial MEP pathways exchange metabolites [20], and hence, linalool could be exclusively synthesized by the MVA pathway as does in strawberry fruit [38]. The production of linalool, the major terpenoid in peach fruit [39], and also detected in the volatile profile of nectarine-*M.*

405 *laxa* interaction [22], varies across time in *Monilinia fructicola*-inoculated peaches, i.e., higher
406 production followed by lower production compared to control fruit along time [40]. Our results
407 show that *PpLIS1* and *PpLIS2* expression in immature resistant 'Venus' fruit was first
408 suppressed in response to *M. laxa* and later activated, probably acting as a defense
409 mechanism. In immature susceptible 'Albared' fruit, the paralog *PpLIS2* was first activated
410 probably as a rapid response to cope against the aggressive pathogen; however, both *PpLIS*
411 decreased thereafter, coinciding with the onset of disease symptoms. In particular, the
412 application of linalool in the culture media (from 0.05 mg mL^{-1} to 0.25 mg mL^{-1}) reduced to
413 around half the *in vitro* growth of three *Monilinia* spp., including *M. laxa* [41]. In this line, our
414 results demonstrated a complete lethal activity of linalool to *M. laxa* when it is applied in the
415 headspace (at 0.11 mg mL^{-1} headspace). This *in vitro* activity, together with the increased
416 expression of linalool biosynthetic genes in the resistant tissue, reveals a potential antifungal
417 role of this compound against *M. laxa.*

418 Results presented herein demonstrated that the different gene expression patterns of the
419 terpenoid biosynthetic pathways among nectarine cultivars with different susceptibility levels
420 to *M. laxa* are dependent on the fruit's ability to activate inducible defenses, potentially, the
421 linalool- and farnesal-related biosynthetic pathways. The flux-direction functions of *HMGR*
422 paralogs associated with the MVA pathway may explain the upregulation of stress-induced
423 genes (e.g., steroids biosynthetic genes) that are involved in biotic stress response, which in
424 turn, can alter other terpenoid pathways (e.g., farnesal-related). Impaired expression of
425 biosynthetic genes related to farnesal and linalool also seemed to be clue in determining the
426 susceptibility to *M. laxa*, since their products have shown to have antifungal properties. This
427 knowledge provides new information regarding the essential terpenoid pathways involved in
428 resistance to *M. laxa*. Further approaches aiming to functionally determine the role of specific
429 terpenoid compounds are encouraged to finally develop new strategies to control brown rot
430 in stone fruit.

431

5. Declaration of competing interest

The authors declare that they have no known competing financial interests or personal relationships that could have appeared to influence the work reported in this paper.

6. Author contributions

Marta Balsells-Llauradó: Conceptualization, Methodology, Formal analysis, Investigation, Writing – original draft, Data curation. **Núria Vall-llaura:** Conceptualization, Methodology, Investigation, Writing- Reviewing and Editing. **Josep Usall:** Supervision, Funding acquisition, Writing- Reviewing and Editing. **Christian J. Silva:** Formal analysis, Data curation, Writing-Reviewing and Editing. **Barbara Blanco-Ulate:** Conceptualization, Methodology, Funding acquisition, Writing- Reviewing and Editing. **Neus Teixidó:** Investigation, Resources, Writing-Reviewing and Editing. **Maria Caballol:** Methodology, Investigation, Writing- Reviewing and Editing. **Rosario Torres:** Conceptualization, Supervision, Project administration, Writing-Reviewing and Editing.

7. Acknowledgements

This work was financed by the Spanish government (MINECO) national project AGL2017-84389-C2-1-R, INIA's doctoral grant CPD2016-0159 (MB-L.), and by the CERCA Programme/Generalitat de Catalunya grants. Start-up funds from the College of Agricultural and Environmental Sciences and the Department of Plant Sciences (UC Davis) was awarded to BB-U. Authors are gratefully acknowledged to Júlia Borràs-Bisa for technical support.

8. References

[1] Biswajit Das, *Prunus* diversity- early and present development: A review, Int. J. Biodivers. Conserv. 3 (2011) 721–734. https://doi.org/10.5897/ijbcx11.003.

[2] M. Shahbandeh, Global fruit production in 2017, by variety, (2019). https://www.statista.com/statistics/264001/worldwide-production-of-fruit-by-variety/

(accessed December 16, 2019).

[3] FAO, Database of Food and Agriculture Organization of the United Nations, (2021). http://www.fao.org/faostat/en/#data/QC/visualize (accessed April 29, 2021).

[4] M.H. Mustafa, D. Bassi, M.-N. Corre, L.O. Lino, V. Signoret, B. Quilot-Turion, M. Cirilli, Phenotyping brown rot susceptibility in stone fruit: A literature review with emphasis on peach, Horticulturae. 7 (2021) 115. https://doi.org/10.3390/horticulturae7050115.

[5] V.I. Obi, J.J. Barriuso, Y. Gogorcena, Peach brown rot: Still in search of an ideal management option, Agriculture. 8 (2018) 1–34. https://doi.org/10.3390/agriculture8080125.

[6] S. Kreidl, J. Edwards, O.N. Villalta, Assessment of pathogenicity and infection requirements of *Monilinia* species causing brown rot of stone fruit in Australian orchards, Australas. Plant Pathol. 44 (2015) 419–430. https://doi.org/10.1007/s13313-015-0362-7.

[7] N. Rungjindamai, P. Jeffries, X.-M. Xu, Epidemiology and management of brown rot on stone fruit caused by *Monilinia laxa*, Eur. J. Plant Pathol. 140 (2014) 1–17. https://doi.org/10.1007/s10658-014-0452-3.

[8] Bulletin OEPP/EPPO, PM 7/18 (3) *Monilinia fructicola*, EPPO Bull. 50 (2020) 5–18. https://doi.org/10.1111/epp.12609.

[9] C. Garcia-Benitez, P. Melgarejo, A. De Cal, B. Fontaniella, Microscopic analyses of latent and visible *Monilinia fructicola* infections in nectarines, PLoS One. 11 (2016) e0160675. https://doi.org/10.1371/journal.pone.0160675.

[10] M. Guidarelli, P. Zubini, V. Nanni, C. Bonghi, A. Rasori, P. Bertolini, E. Baraldi, Gene expression analysis of peach fruit at different growth stages and with different susceptibility to *Monilinia laxa*, Eur. J. Plant Pathol. 140 (2014) 503–513. https://doi.org/10.1007/s10658-014-0484-8.

[11] Y. Luo, T.J. Michailides, D.P. Morgan, W.H. Krueger, R.P. Buchner, Inoculum dynamics, fruit infection, and development of brown rot in prune orchards in California, Phytopathology. 95 (2005) 1132–1136. https://doi.org/10.1094/PHYTO-95-1132.

[12] M. Balsells-Llauradó, C.J. Silva, J. Usall, N. Vall-llaura, S. Serrano-Prieto, N. Teixidó, S.D. Mesquida-Pesci, A. de Cal, B. Blanco-Ulate, R. Torres, Depicting the battle between nectarine and *Monilinia laxa*: the fruit developmental stage dictates the effectiveness of the host defenses and the pathogen's infection strategies, Hortic. Res. 7 (2020) 1–15. https://doi.org/10.1038/s41438-020-00387-w.

[13] N. Alkan, A.M. Fortes, Insights into molecular and metabolic events associated with fruit response to post-harvest fungal pathogens, Front. Plant Sci. 6 (2015) 889. https://doi.org/10.3389/fpls.2015.00889.

[14] H. Liu, X. Cao, X. Liu, R. Xin, J. Wang, J. Gao, B. Wu, L. Gao, C. Xu, B. Zhang, D. Grierson, K. Chen, UV-B irradiation differentially regulates terpene synthases and terpene content of peach, Plant Cell Environ. 40 (2017) 2261–2275. https://doi.org/10.1111/pce.13029.

[15] S. Khare, N.B. Singh, A. Singh, I. Hussain, K. Niharika, V. Yadav, C. Bano, R.K. Yadav, N. Amist, Plant secondary metabolites synthesis and their regulations under biotic and abiotic constraints, J. Plant Biol. 63 (2020) 203–216. https://doi.org/10.1007/s12374-020-09245-7.

[16] B. Blanco-Ulate, K.C. Amrine, T.S. Collins, R.M. Rivero, A.R. Vicente, A. Morales-Cruz, C.L. Doyle, Z. Ye, G. Allen, H. Heymann, S.E. Ebeler, D. Cantu, Developmental and metabolic plasticity of white-skinned grape berries in response to *Botrytis cinerea* during noble rot, Plant Physiol. 169 (2015) pp.00852.2015. https://doi.org/10.1104/pp.15.00852.

[17] B. Quilot-Turion, M.-N. Corre, G. Costagliola, L. Heurtevin, V. Signoret, M.D.C. Raseira, M.D. Vinoly, Wounding nectarine fruit disrupts *Monilinia laxa* infection: deciphering fruit gene pathway involved and the role of phenolic and volatile compounds, in: 10th Rosaceae Genomics Conf., Barcelona, Spain, 2020. hal-03267785%0AHAL (accessed July 5, 2021).

[18] D. Tholl, Biosynthesis and biological functions of terpenoids in plants, Adv. Biochem. Eng. Biotechnol. 148 (2015) 63–106. https://doi.org/10.1007/10_2014_295.

[19] J. Chang, Y. Ning, F. Xu, S. Cheng, X. Li, Research advance of 3-hydroxy-3-methylglutaryl-coenzyme a synthase in plant isoprenoid biosynthesis, J. Anim. Plant Sci. 25 (2015) 1441–1450.

[20] A. Hemmerlin, J.L. Harwood, T.J. Bach, A raison d'être for two distinct pathways in the early steps of plant isoprenoid biosynthesis?, Prog. Lipid Res. 51 (2012) 95–148. https://doi.org/10.1016/j.plipres.2011.12.001.

[21] L.M. Lois, M. Rodríguez-Concepción, F. Gallego, N. Campos, A. Boronat, Carotenoid biosynthesis during tomato fruit development: Regulatory role of 1-deoxy-D-xylulose 5-phosphate synthase, Plant J. 22 (2000) 503–513. https://doi.org/10.1046/j.1365-313X.2000.00764.x.

[22] M. Balsells-Llauradó, G. Echeverría, R. Torres, N. Vall-llaura, N. Teixidó, J. Usall, Emission of volatile organic compounds during nectarine-*Monilinia laxa* interaction and its relationship with fruit susceptibility to brown rot, Postharvest Biol. Technol. 192 (2022). https://doi.org/10.1016/J.POSTHARVBIO.2022.111997.

[23] N. Baró-Montel, R. Torres, C. Casals, N. Teixidó, J. Segarra, J. Usall, Developing a methodology for identifying brown rot resistance in stone fruit, Eur. J. Plant Pathol. 154 (2019) 287–303. https://doi.org/10.1007/s10658-018-01655-1.

[24] N. Baró-Montel, N. Vall-llaura, J. Usall, N. Teixidó, M.A. Naranjo-Ortíz, T. Gabaldón, R. Torres, Pectin methyl esterases and rhamnogalacturonan hydrolases: weapons for successful *Monilinia laxa* infection in stone fruit?, Plant Pathol. 68 (2019) 1381–93. https://doi.org/10.1111/ppa.13039.

[25] Z. Tong, Z. Gao, F. Wang, J. Zhou, Z. Zhang, Selection of reliable reference genes for gene expression studies in peach using real-time PCR, BMC Mol. Biol. 10 (2009) 1–13. https://doi.org/10.1186/1471-2199-10-71.

[26] M.W. Pfaffl, A new mathematical model for relative quantification in real-time RT-PCR., Nucleic Acids Res. 29 (2001) 45e – 45. https://doi.org/10.1093/nar/29.9.e45.

[27] S. Cao, M. Liang, L. Shi, J. Shao, C. Song, K. Bian, W. Chen, Z. Yang, Accumulation of carotenoids and expression of carotenogenic genes in peach fruit, Food Chem. 214

(2017) 137–146. https://doi.org/10.1016/j.foodchem.2016.07.085.

[28] A. Muto, C.T. Müller, L. Bruno, L. McGregor, A. Ferrante, A.A.C. Chiappetta, M.B. Bitonti, H.J. Rogers, N.D. Spadafora, Fruit volatilome profiling through GC × GC-ToF-MS and gene expression analyses reveal differences amongst peach cultivars in their response to cold storage, Sci. Reports 2020 101. 10 (2020) 1–16. https://doi.org/10.1038/s41598-020-75322-z.

[29] C. Garcia-Benitez, C. Casals, J. Usall, I. Sánchez-Ramos, P. Melgarejo, A. De Cal, Impact of postharvest handling on preharvest latent infections caused by *Monilinia* spp. in nectarines, J. Fungi. 6 (2020) 1–14. https://doi.org/10.3390/jof6040266.

[30] S. Taniguchi, S. Miyoshi, D. Tamaoki, S. Yamada, K. Tanaka, Y. Uji, S. Tanaka, K. Akimitsu, K. Gomi, Isolation of jasmonate-induced sesquiterpene synthase of rice: Product of which has an antifungal activity against *Magnaporthe oryzae*, J. Plant Physiol. 171 (2014) 625–632. https://doi.org/10.1016/J.JPLPH.2014.01.007.

[31] Z.M. Haile, E.G. Nagpala-De Guzman, M. Moretto, P. Sonego, K. Engelen, L. Zoli, C. Moser, E. Baraldi, Transcriptome profiles of strawberry (*Fragaria vesca*) fruit interacting with *Botrytis cinerea* at different ripening stages, Front. Plant Sci. 10 (2019). https://doi.org/10.3389/fpls.2019.01131.

[32] M. Rodríguez-Concepción, W. Gruissem, Arachidonic acid alters tomato *HMG* expression and fruit growth and induces 3-hydroxy-3-methylglutaryl coenzyme A reductase-independent lycopene accumulation, Plant Physiol. 119 (1999) 41–48. https://doi.org/10.1104/pp.119.1.41.

[33] T. Griebel, J. Zeier, A role for β-sitosterol to stigmasterol conversion in plant-pathogen interactions, Plant J. 63 (2010) 254–268. https://doi.org/10.1111/j.1365-313X.2010.04235.x.

[34] P. Agudelo-Romero, A. Erban, C. Rego, P. Carbonell-Bejerano, T. Nascimento, L. Sousa, J.M. Martínez-Zapater, J. Kopka, A.M. Fortes, Transcriptome and metabolome reprogramming in *Vitis vinifera* cv. Trincadeira berries upon infection with *Botrytis cinerea*, J. Exp. Bot. 66 (2015) 1769–1785. https://doi.org/10.1093/jxb/eru517.

572 [35] M. Nagaki, T. Narita, H. Ichikawa, J. Kawakami, A. Nakane, Antibacterial and antifungal
573 activities of isoprenoids, Trans. Mater. Res. Soc. Japan. 36 (2011) 55–58.
574 [36] I.J. Biva, C.P. Ndi, S.J. Semple, H.J. Griesser, Antibacterial performance of terpenoids
575 from the australian plant *Eremophila lucida*, Antibiotics. 8 (2019) 6–11.
576 https://doi.org/10.3390/antibiotics8020063.
577 [37] M. Cantó-Tejero, J.L. Casas, M.Á. Marcos-García, M.J. Pascual-Villalobos, V.
578 Florencio-Ortiz, P. Guirao, Essential oils-based repellents for the management of
579 *Myzus persica*e and *Macrosiphum euphorbiae*, J. Pest Sci. (2004). 1 (2021) 1–15.
580 https://doi.org/10.1007/s10340-021-01380-5.
581 [38] D. Hampel, A. Mosandl, M. Wüst, Biosynthesis of mono- and sesquiterpenes in
582 strawberry fruits and foliage: ^{2}H labeling studies, J. Agric. Food Chem. 54 (2006) 1473–
583 1478. https://doi.org/10.1021/jf0523972.
584 [39] Y.J. Wang, C.X. Yang, S.H. Li, L. Yang, Y.N. Wang, J.B. Zhao, Q. Jiang, Volatile
585 characteristics of 50 peaches and nectarines evaluated by HP-SPME with GC-MS,
586 Food Chem. 116 (2009) 356–364. https://doi.org/10.1016/j.foodchem.2009.02.004.
587 [40] Q. Liu, N. Zhao, D. Zhou, Y. Sun, K. Sun, L. Pan, K. Tu, Discrimination and growth
588 tracking of fungi contamination in peaches using electronic nose, Food Chem. 262
589 (2018) 226–234. https://doi.org/10.1016/j.foodchem.2018.04.100.
590 [41] H.S. Elshafie, E. Mancini, S. Sakr, L. De Martino, C.A. Mattia, V. De Feo, I. Camele,
591 Antifungal activity of some constituents of *Origanum vulgare* L. essential oil against
592 postharvest disease of peach fruit, J. Med. Food. 18 (2015) 929–934.
593 https://doi.org/10.1089/jmf.2014.0167.
594 [42] F. Supek, M. Bošnjak, N. Škunca, T. Šmuc, Revigo summarizes and visualizes long
595 lists of gene ontology terms, PLoS One. 6 (2011).
596 https://doi.org/10.1371/JOURNAL.PONE.0021800.
597

598 **Tables**

599 **Table 1. Antifungal activity of linalool and farnesol at different concentrations (mg L^{-1}**
600 **headspace or culture media, respectively) on the *in vitro* growth of *M. laxa.***
601 Measurements correspond to 3 days and 7 days (corresponding to 3 days with the presence
602 of the compound followed by 4 days in absence of the compound). Different letters indicate
603 significant differences ($P \leq 0.05$) of growth inhibition among tested concentration for each time
604 point. Values represent the mean and the standard error of the means of the two experiments
605 conducted.

606

	Concentration (mg mL^{-1})	*M. laxa* growth inhibition (%)	
		3 days	7 days
Linalool	0.11	100.0 ± 0 a	100.0 ± 0 a
	0.05	89.3 ± 4.8 ab	19.9 ± 5.6 b
	0.03	80.0 ± 3.0 bc	2.9 ± 2.3 c
	0.01	68.2 ± 4.7 c	0 ± 0 c
Farnesol	0.89	84.2 ± 1 a	0.0
	0.44	81.6 ± 1.2 a	0.0
	0.22	67.2 ± 2.8 ab	0.0
	0.11	47.3 ± 2 bc	0.0
	0.06	41.4 ± 0 c	0.0

607

608

Table 2. Representation of log_2FC between inoculated and control tissues for each cultivar, developmental stage, and time point for *PpPFT1, PpSIMT, PpFOLK, PpLIS1*, and *PpLIS2*, the key genes described in this study to be important for brown rot progression. Values used to calculate the log_2FC were taken from the normalized read counts and relative expression for 'Venus' (Figure 3 and Suppl. Table S3) and 'Albared' (Figures 6 and 7), respectively. Bold values indicate significant differences between inoculated and control tissues (according to Figures 3, 6, and 7). Red or green values indicate upregulation or downregulation, respectively, for inoculated tissues compared to control.

			PpPFT1	*PpSIMT*	*PpFOLK*	*PpLIS1*	*PpLIS2*	
'Venus'	**Immature**	**6 hpi**	0,1	-0,1	-0,2	**-1,1**	**-0,6**	resistant tissue
		14 hpi	-0,4	0,2	**0,4**	**0,7**	**0,3**	
		24 hpi	-0,1	-0,1	-0,3	**0,5**	-0,1	
		48 hpi	0,0	0,0	0,1	0,5	**0,5**	
	Mature	**6 hpi**	0,0	0,0	0,1	**0,7**	0,1	susceptible tissues
		14 hpi	-0,3	-0,1	0,0	0,2	0,1	
		24 hpi	**-0,5**	-0,1	-0,3	**0,7**	**-0,7**	
		48 hpi	**-0,7**	**-0,7**	**-0,6**	0,3	**-1,2**	
'Albared'	**Immature**	**6 hpi**	**-0,76**	-1,12	-0,37	-0,19	-0,27	
		14 hpi	0,22	2,34	-0,29	0,48	**1,09**	
		24 hpi	-0,19	-0,35	-0,34	0,16	0,79	
		48 hpi	0,50	-0,12	**-0,84**	0,48	**-0,95**	
		72 hpi	**-1,62**	-4,18	**-2,78**	**-0,84**	**-2,67**	
	Mature	**6 hpi**	**0,49**	1,24	0,30	**1,46**	0,15	
		14 hpi	-0,23	0,78	-0,12	0,55	0,07	
		24 hpi	**-1,53**	-2,27	**-1,21**	-0,34	**-1,74**	
		48 hpi	**-1,23**	-0,91	**-1,30**	0,65	-0,88	
		72hpi	0,65	0,11	-0,32	-0,99	0,53	

Figures

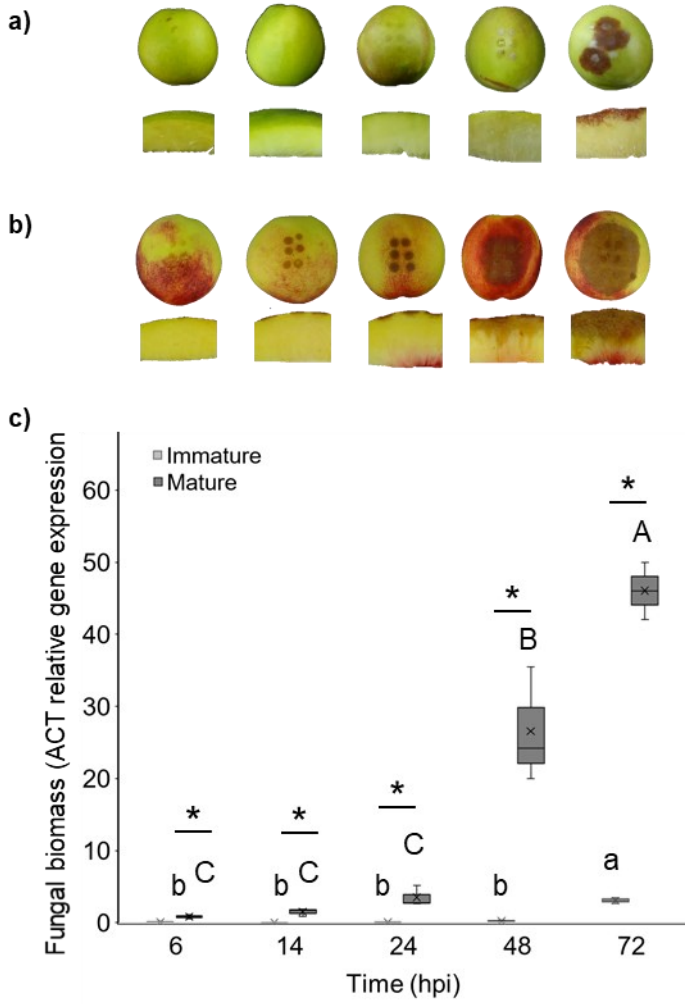

Figure 1. Brown rot progression and *M. laxa* biomass in 'Albared' nectarines. Images (entire fruit and perpendicular section) display brown rot development in immature (a) and mature (b) tissues along hours post inoculation (hpi). (c) Assessment of *M. laxa* biomass by relative gene expression of *M. laxa ACTIN* (*MlACT*) reference gene, normalized to nectarine *ELONGATION FACTOR 2* (*PpTEF2*) reference gene in both stages, immature (light grey) and mature (dark grey) of *M. laxa*-inoculated fruit. The box plot represents the mean of three biological replicates consisting of five fruit each with its interquartile range. Lowercase and uppercase letters indicate significant differences across time ($P \leq 0.05$, Tukey's test) in immature and mature tissues, respectively. Asterisks indicate significant differences between stages at each time point ($P \leq 0.05$, Student's *T* test). Brown rot progression in 'Venus' nectarines can be found in our previous study [12].

634

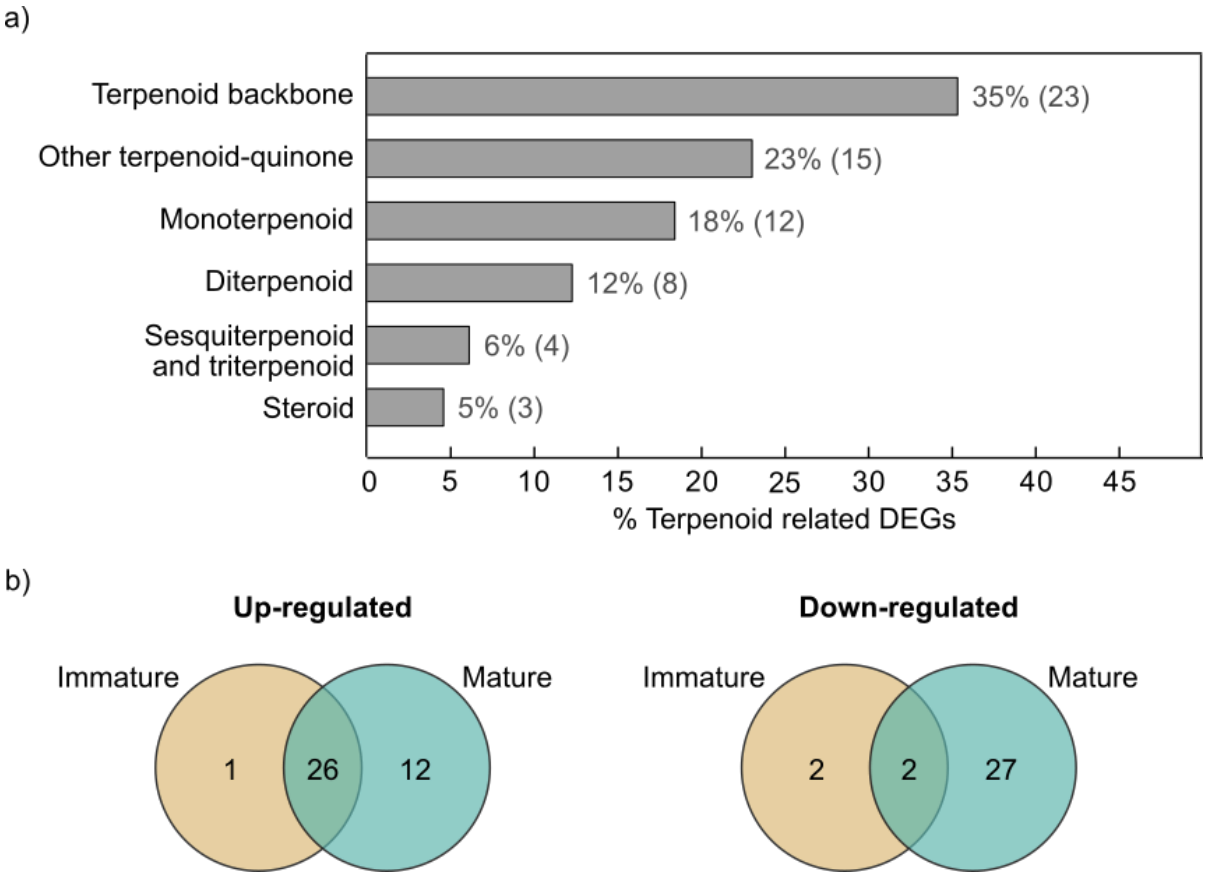

635

636

637 **Figure 2. Analyses of RNA-Seq data of 'Venus' nectarines.** A) Terpenoid-related families
638 for nectarine differentially expressed genes (DEGs) (between control and inoculated) based
639 on KEGG (Kyoto Encyclopedia of Genes and Genomes) in cv. 'Venus'. Each category is
640 represented by the proportion (%) of annotated transcripts for all terpenoid-related DEGs, and
641 the specific number of DEGs in brackets. B) Venn's diagram of nectarine terpenoid-related
642 DEGs representing the common and unique DEGs between developmental stages (immature
643 and mature) for up and down-regulated genes. Data of this figure is obtained from our
644 previous RNA-Seq study [12].

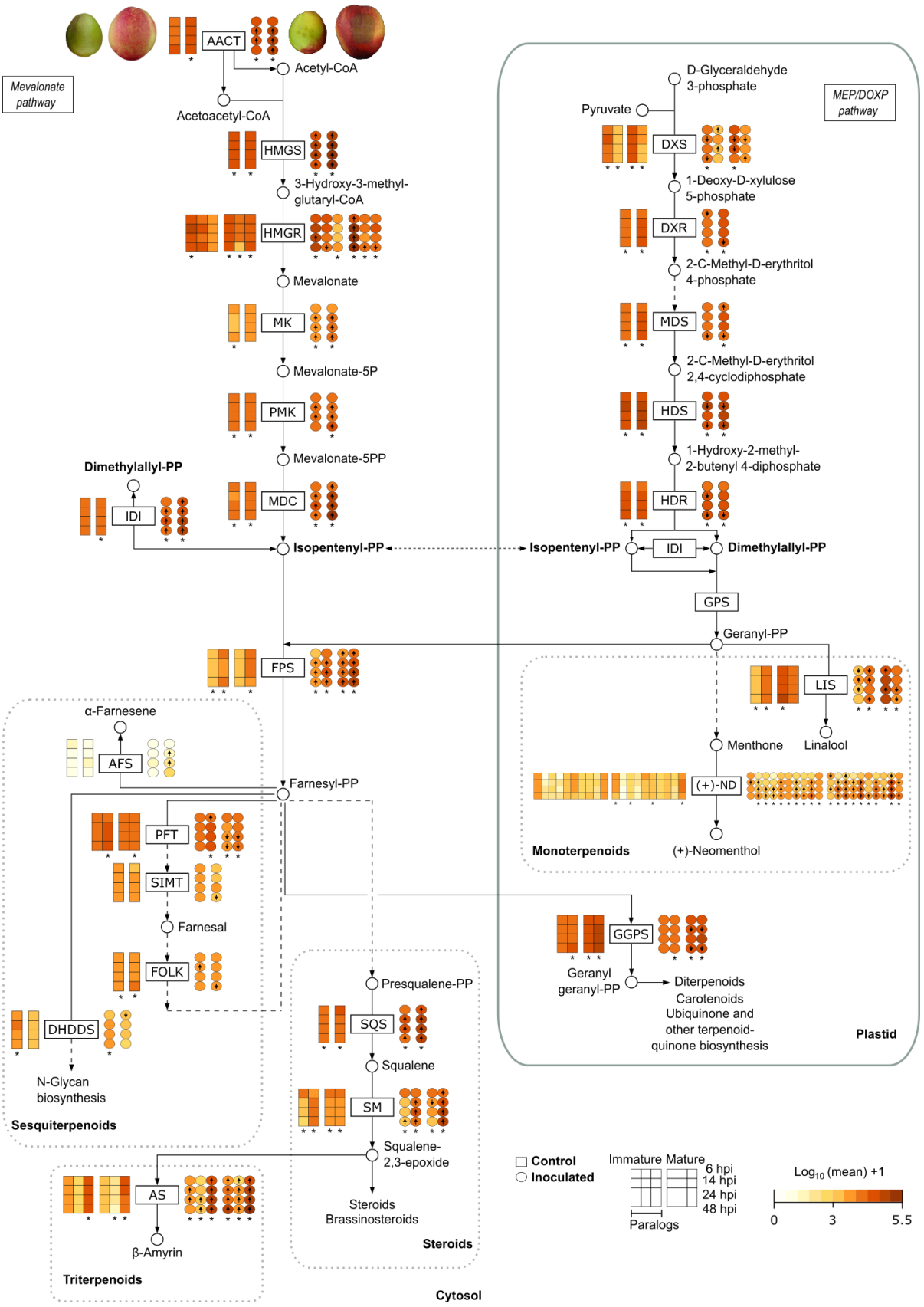

Figure 3. Expression of terpenoid pathway in control and *M. laxa*-inoculated 'Venus' nectarine at immature and mature stages. The terpenoid biosynthetic pathway is shown

649 with substrates (cercles) and enzymes (enzyme name inside boxes) and includes 42
650 differentially expressed genes based on previous studies [12]. The scale color of the heat
651 map represents the intensity of the mean of normalized read counts, expressed as $Log_{10} + 1$.
652 The normalized read counts expression is represented for control (□) and inoculated (o)
653 tissues for each immature (left) and mature (right) stage at each time point after inoculation
654 (hpi). Multiple columns of the same gene represent different gene paralogs. Dashed lines
655 indicated that some steps had been omitted. Up or down black arrows on circles represent
656 significantly higher or lower normalized read counts for the inoculated tissues compared to
657 control fruit for each time point, stage, and gene ($P \leq 0.05$, Student's T test). Asterisks indicate
658 significant differences across time for each gene, tissue, and stage ($P \leq 0.05$, Tukey's test).
659 Enzyme abbreviations, corresponding gene accessions and details of statistical analysis are
660 provided in **Suppl. Table S3**. Fruit images correspond to immature and mature stages of
661 control (left) and inoculated (right) tissues at 48 hpi [12], licensed under a Creative Commons
662 Attribution 4.0 International License (CC BY 4.0).
663
664

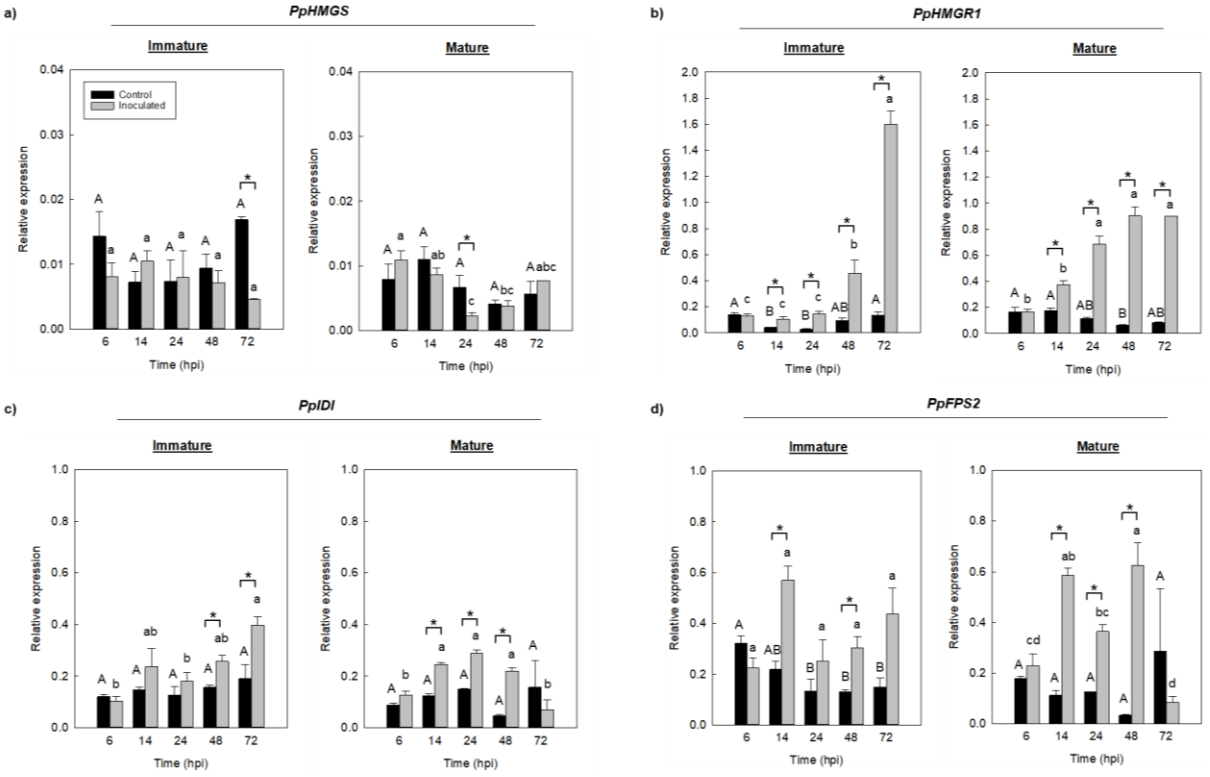

Figure 4. Relative expression of four genes of the terpenoid backbone pathway in the 'Albared' cultivar. a) *PpHMGS* (Hydroxymethylglutaryl-CoA synthase); b) *PpHMGR1* (Hydroxymethylglutaryl-CoA reductase); c) *PpIDI* (Isopentenyl-diphosphate delta-isomerase); d) *PpFPS2* (Farnesyl diphosphate synthase / farnesyl pyrophosphate synthase). Asterisks indicate significant differences between control and inoculated tissues for each developmental stage (immature and mature) at each time point ($P \leq 0.05$, Student's *T* test). Different uppercase (A-D) and lowercase (a-d) letters indicate significant differences across time ($P \leq 0.05$, Tukey's test) for each control and inoculated immature or mature tissues, respectively. Values represent the mean and error bars represent the standard error of the means (n = 3).

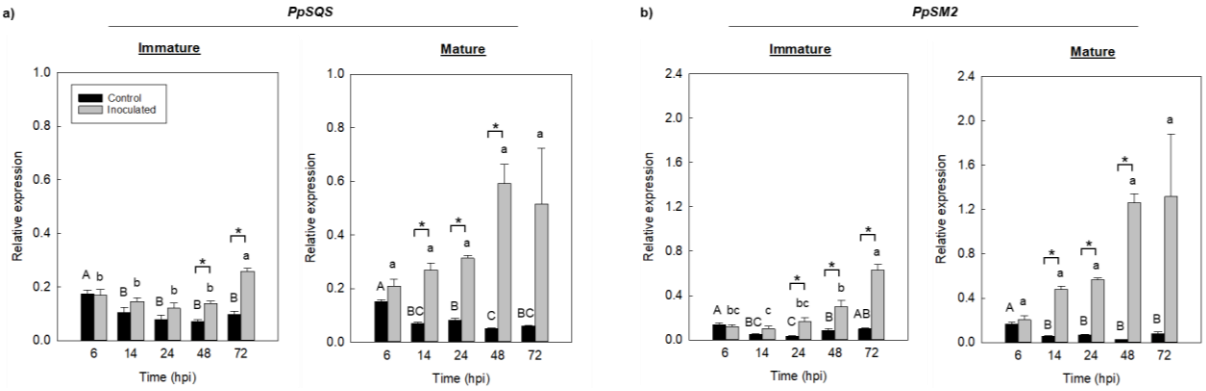

Figure 5. Relative expression of steroid biosynthetic genes in the 'Albared' cultivar. a) *PpSQS* (Squalene synthase / Farnesyl-diphosphate farnesyltransferase); b) *PpSM2* (Squalene monooxygenase). Asterisks indicate significant differences between control and inoculated tissues for each developmental stage (immature and mature) at each time point ($P \leq 0.05$, Student's *T* test). Different uppercase (A-D) and lowercase (a-d) letters indicate significant differences across time ($P \leq 0.05$, Tukey's test) for each control and inoculated immature or mature tissues, respectively. Values represent the mean and error bars represent the standard error of the means (n = 3).

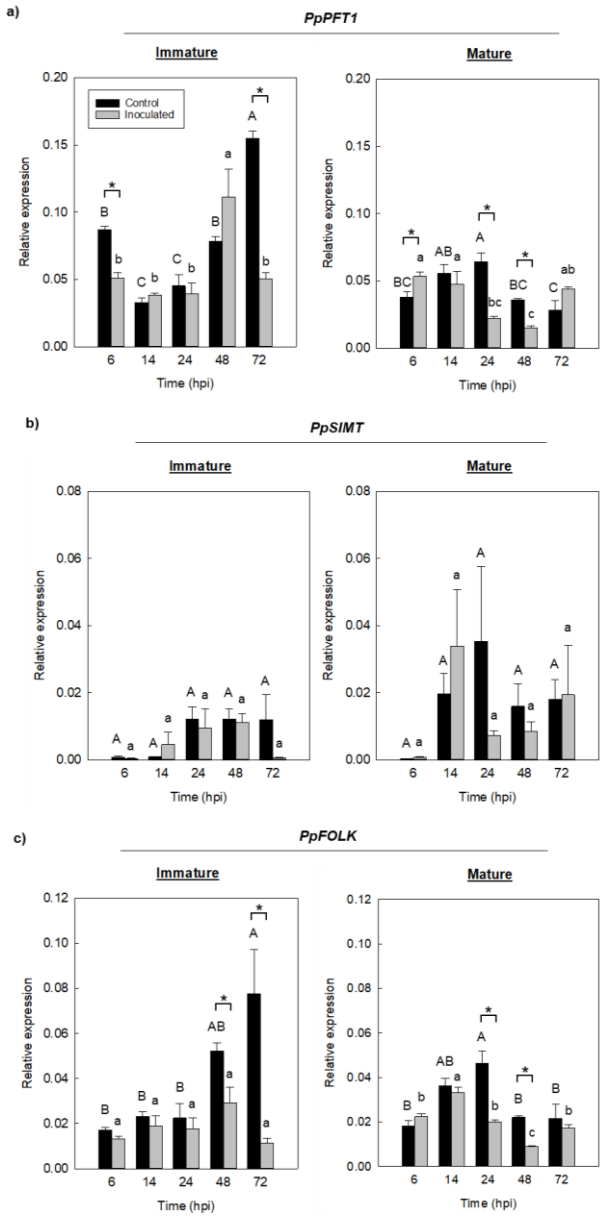

Figure 6. Relative expression of farnesal biosynthetic genes in the 'Albared' cultivar. a) *PpPFT* (Protein farnesyltransferase subunit beta); b) *PpSIMT* (Protein-S-isoprenylcysteine O-methyltransferase); c) *PpFOLK* (Farnesol kinase). Asterisks indicate significant differences between control and inoculated tissues for each developmental stage (immature and mature) at each time point ($P \leq 0.05$, Student's *T* test). Different uppercase (A-D) and lowercase (a-d) letters indicate significant differences across time ($P \leq 0.05$, Tukey's test) for each control and inoculated immature or mature tissues, respectively. Values represent the mean and error bars represent the standard error of the means (n = 3).

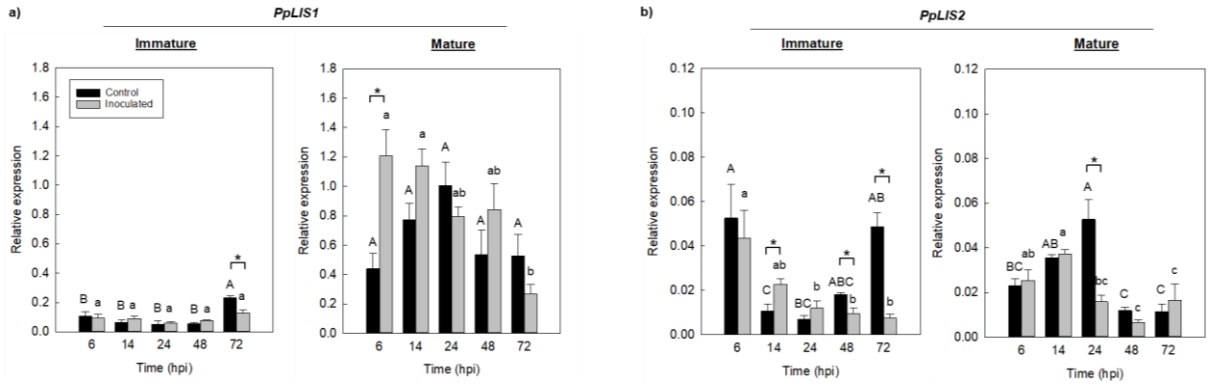

Figure 7. Expression of linalool biosynthetic genes in the 'Albared' cultivar. Two paralogs of the 3S-linalool synthase gene, *PpLIS1* (a) and *PpLIS2* (b). Asterisks indicate significant differences between control and inoculated tissues for each developmental stage (immature and mature) at each time point ($P \leq 0.05$, Student's *T* test). Different uppercase (A-D) and lowercase (a-d) letters indicate significant differences across time ($P \leq 0.05$, Tukey's test) for each control and inoculated immature or mature tissues, respectively. Values represent the mean and error bars represent the standard error of the means (n = 3).

Supplementary Material

Tables

Supplementary Table S1: List of the primers used for RT-qPCR. From left to right: Target Gene, Gene Abbreviation, Transcript Accession, Reference, Type, Primer Sequence (5´-3') and Primer efficiency (%). Reference or de novo design is also specified.

Supplementary Table S2: Pearson's correlation between RNA-Seq (normalized read counts) and relative expression (RT-qPCR) of 'Venus' cultivar. Values represent the mean (n = 3) of expression values for each stage, tissue, and time point.

Supplementary Table S3: Gene accession, enzyme name and abbreviation of genes related to terpenoid pathway (tab 1) and details of statistical analysis of normalized read counts of 'Venus' cultivar (tab 2).

Figures

Supplementary Figure S1. Evaluation of *M. laxa* infection on immature and mature 'Venus' nectarines at 48 hours post inoculation [12], licensed under a Creative Commons Attribution 4.0 International License (CC BY 4.0).